

Magnetic nanoparticles coated with immobilized alkaline phosphatase for enzymolysis and enzyme inhibition assays†

Cite this: *J. Mater. Chem. B*, 2013, **1**, 1749

Siming Wang, Ping Su, Jun Huang, Jingwei Wu and Yi Yang*

Magnetic nanoparticles are potentially useful as supports for biomacromolecules because of their biocompatibility, low toxicity and easy separation. In this study, alkaline phosphatase (ALP) was used as a model enzyme, and a new type of immobilized ALP was prepared on superparamagnetic nanoparticles and confirmed by various characterization techniques. X-ray diffraction (XRD), scanning electron microscopy (SEM) and vibrating sample magnetometry (VSM) results present that the synthesized nanoparticles possess a clear three-dimensional core-shell architecture with an average diameter of about 390 nm and a high saturation magnetization of 86.7 emu g⁻¹. Fourier-transform infrared spectra (FTIR) and thermogravimetric analysis (TGA) results show that ALP was successfully attached to the surface of magnetic nanoparticles via a crosslinking technique. An enzyme inhibition study was performed on the immobilized ALP magnetic nanoparticles using theophylline, L-tryptophan and D-tryptophan as model inhibitors. The enzyme kinetics indicate that D-tryptophan possesses chiral discrimination inhibition and L-tryptophan exhibits uncompetitive inhibition for ALP, compared with no obvious inhibition observed with its enantiomer. The results also show that theophylline is a noncompetitive inhibitor and has a markedly higher inhibitory effect than L-tryptophan. The protocol described allows easy manipulation, reduces procedural time and can be adapted to high-throughput screening of enzyme reactions and inhibitors.

Received 21st December 2012

Accepted 29th January 2013

DOI: 10.1039/c3tb00562c

www.rsc.org/MaterialsB

1 Introduction

Magnetic nanoparticles are advanced materials that have potential use as supports for biomacromolecules, such as nucleic acids, antibodies, peptides and enzymes.^{1–5} Magnetic nanoparticles with immobilized enzymes or proteins possess several notable advantages due to their novel nanostructures and magnetic properties. Such nanoparticles can provide a biocompatible and inert microenvironment that does not interfere with the native properties of enzymes or proteins, thus retaining their biological activities.⁶ Their nanoscale structures reduce diffusion limitations and offer a large specific surface area, resulting in a low mass transfer resistance and high binding capacity. In addition, sensitive magnetic responses enable easy separation of immobilized enzymes or proteins from reaction mixtures simply by applying a magnetic field, with no need for centrifuges, filters or other equipment, which significantly shortens procedural time and simplifies the experimental process.^{7,8} Furthermore, these functionalized

magnetic nanoparticles are compatible with multiple approaches, allowing the coupling of various analytical techniques such as mass spectrometry and capillary electrophoresis.^{9–11} Because of these unique properties and functions, immobilized enzymes or proteins on magnetic nanoparticles show great promise for applications in liquid-phase reactions, especially in the fields of biocatalysis,¹² biosensors,¹³ biological recognition¹⁴ and biological screening.¹⁵

Alkaline phosphatase (ALP) is a nonspecific phosphomonoesterase found widely in many mammalian tissues.¹⁶ It is involved in various metabolic functions such as fat absorption, mucosal defense and skeletal mineralization, to catalyze the hydrolysis of phosphomonoesters, releasing free inorganic phosphate and alcohol.^{17,18} ALP is often used as a major target in analytical chemistry, biochemistry and medical chemistry to probe causative disease mechanisms. Studies of ALP activity and screening of its inhibitors are required in clinical diagnostics to develop potential drug therapies for osteoarthritis, idiopathic infantile arterial calcification and end-stage renal diseases.^{19,20} However, many ALP assays use free enzyme in a homogeneous solution, which may be susceptible to denaturation and is difficult to reuse or recover, leading to high cost and sample complexity. Moreover, free enzyme is possibly limited through spectrophotometric interferences arising from self-absorption. Immobilized enzymes can not only retain a major enzymatic

College of Science, Beijing University of Chemical Technology, Beijing 100029, P.R. China. E-mail: yangyi@mail.buct.edu.cn; Fax: +86-10-64434898; Tel: +86-10-64454599

† Electronic supplementary information (ESI) available. See DOI: 10.1039/c3tb00562c

activity but also improve stability compared with free enzymes.^{21,22} They have potential applications in the fields of biochemistry, food, clinical diagnosis and environmental engineering.^{23–26} Therefore, a simple, efficient and economic immobilized ALP is needed for enzymatic and inhibitory assays of ALP.

This current study focuses on developing a new type of immobilized ALP using superparamagnetic nanoparticles. Aminated silica-coated Fe₃O₄ magnetite particles were synthesized through a solvent-thermal method, characterized by various analytical techniques, and applied to immobilization of ALP. This immobilized enzyme offers the advantages of easy isolation, low cost and high efficiency. Optimal enzymolysis conditions for applying the immobilized ALP magnetic nanoparticles, including temperature, incubation time, pH and substrate concentration, were identified by high performance liquid chromatography (HPLC). The other enzymatic parameters of the immobilized ALP, such as the Lineweaver–Burk plot and Michaelis constant as well as repeatability and stability, were also evaluated. Finally, theophylline, L-tryptophan and D-tryptophan were used as model inhibitors, and an enzyme inhibition study was performed on the immobilized ALP magnetic nanoparticles to confirm their performance in enzyme assays.

2 Materials and methods

2.1 Chemicals and materials

ALP (EC 3.1.3.1 from *bovine intestinal mucosa*, 10 U mg⁻¹) and 4-nitrophenylphosphate were purchased from Sigma-Aldrich (St Louis, MO, USA). Theophylline and 4-nitrophenol were obtained from AccuStandard (New Haven, CT, USA). γ -Aminopropyltriethoxysilane (APES), sodium cyanoborohydride and D-tryptophan were obtained from Acros Organics (Geel, Belgium). L-Tryptophan, tetraethoxysilane and methanol (HPLC grade) were purchased from J&K Scientific (Beijing, China). Magnesium chloride, zinc chloride, iron(III) chloride hexahydrate, sodium acetate and glycol were supplied by Beijing Yili Chemical (Beijing, China). All other chemical reagents used in the experiment were of analytical grade.

2.2 Instrumentation

HPLC analyses were performed on an Agilent 1100 Series HPLC system (Agilent, Santa Clara, CA, USA) equipped with an Agilent Eclipse XDB-C18 column (150 × 4.6 mm, i.d., 5 μ m particle) at room temperature and an ultraviolet detector operated at 311 nm wavelength. The mobile phase was methanol : water (40% : 60%, v/v) with a flow rate of 1.0 ml min⁻¹. Agilent LC ChemStation software was used for system control, data collection and processing. X-ray diffraction patterns (XRD) were collected on a D/max-Ultima (Rigaku, Tokyo, Japan) using Cu K α radiation (40 kV, 40 mA, $\lambda = 1.5418 \text{ \AA}$) with a scan step of 0.02°. The sizes and morphologies of magnetic nanoparticles were tested using a transmission electron microscope (TEM, Hitachi H800, Tokyo, Japan). The magnetic properties of the prepared nanoparticles were measured on a vibrating sample magnetometer (VSM, Lake Shore 7410, Westerville, OH, USA). Fourier-transform infrared spectra (FTIR) were obtained using a

Thermo Scientific Nicolet 8700 (Waltham, MA, USA). Thermogravimetric analysis (TGA) was performed for powdered samples with a heating rate of 10 °C min⁻¹ from room temperature to 800 °C under a nitrogen atmosphere using a HCT-2 thermo analysis system (Beijing Henven Scientific Instrument Corporation, Beijing, China).

2.3 Preparation of core-shell structured Fe₃O₄@SiO₂@APES nanoparticles

Aminated silica-coated magnetic nanoparticles were synthesized sequentially through a solvothermal reaction, sol-gel coating approach and silanization process.^{27,28} In brief, 1.35 g of FeCl₃·6H₂O as a single ferric source and 3.6 g of sodium acetate were dissolved in 40 ml of glycol under vigorous stirring for 30 min. The obtained homogenous yellow solution was transferred into a Teflon-lined stainless-steel autoclave, sealed, and heated at 200 °C for 8 h. The resulting black magnetite particles were separated with an external magnet, washed with ethanol and water several times, and vacuum dried for 4 h. Next, the sol-gel approach was applied to preparing core-shell structured Fe₃O₄@SiO₂. The Fe₃O₄ nanobeads were dispersed in a solution of ethanol (150 ml), deionized water (50 ml) and concentrated ammonia aqueous solution (5 ml, 28 wt%), followed by dropwise addition of 50 ml of ethanol containing 2 ml of tetraethoxysilane with stirring for 6 h. Subsequently, the silica-coated Fe₃O₄ was collected with a magnet and washed sequentially with 1 M HCl, water and ethanol. After vacuum drying, Fe₃O₄@SiO₂ was mixed with a 10% (v/v) APES toluene solution at 100 °C for 24 h under inert conditions using nitrogen. Finally, the Fe₃O₄@SiO₂@APES beads were separated, washed with ethanol, and dried in a vacuum.

2.4 ALP immobilization

After washing with 20 mM pH 8.5 carbonate buffer, the Fe₃O₄@SiO₂@APES nanoparticles were reacted with 5% glutaraldehyde solution for 1 h and then washed with carbonate buffer. Thereafter, the magnetic nanoparticles were immersed in a 2.5 mg ml⁻¹ ALP and sodium cyanoborohydride carbonate solution (pH 8.5) and incubated for 2 h. Sodium cyanoborohydride reduces the Schiff base and promotes the formation of stable secondary amine linkages between the immobilized enzyme and magnetite. Finally, the immobilized ALP magnetic nanoparticles, rinsed with carbonate buffer, were stored at 4 °C until use. In this way, ALP was covalently attached to the surface of the magnetic nanoparticles.

2.5 Immobilized enzyme activity assay and inhibition study

An enzymatic hydrolysis reaction was chosen for the immobilized ALP magnetic nanoparticles based on 4-nitrophenylphosphate as a substrate. The corresponding enzymolysis product was 4-nitrophenol.²⁹ Due to strong ultraviolet absorbance, both the substrate and product can be monitored spectrophotometrically without requiring derivation. The immobilized ALP magnetic nanoparticles (10 mg) and substrate, in the presence or absence of inhibitors, were mixed and incubated in an enzyme assay buffer (20 mM carbonate buffer containing 5 mM MgCl₂ and 1 mM

ZnCl₂) at a final volume of 10 ml. A magnet was used to gather and isolate the nanospheres, and 20 μl of supernatant was injected into the HPLC. The optimal enzymolysis conditions were obtained according to the peak area of 4-nitrophenol. For the inhibition study, the inhibition percentage was calculated according to the reduction of the product peak area. The procedures for preparing immobilized ALP magnetic nanoparticles and carrying out the enzyme assay are shown schematically in Fig. 1.

3 Results and discussion

3.1 Characterization of immobilized ALP magnetic nanoparticles

The crystalline structure and phase purity were determined by power X-ray diffraction (ESI, Fig. S1†). The diffraction peaks in curves can be assigned to the (2 2 0), (3 1 1), (4 0 0), (4 2 2), (5 1 1) and (4 4 0) planes, and confirmed that the products were well crystallized and indexed as the typical cubic iron oxide Fe₃O₄ (JCPDS card no. 65-3107). There was no obvious change after coating with the SiO₂ layer and silanization, indicating the amorphous nature of the silica shell.

The size and internal structure of magnetic nanoparticles were investigated by TEM. Fig. 2A shows that these Fe₃O₄ magnetite particles had a mean diameter of about 350 nm and consisted of many nanoparticles with an average crystallite size of 16 nm, calculated from the X-ray diffraction results according to the Scherrer equation, similar to the results reported in the

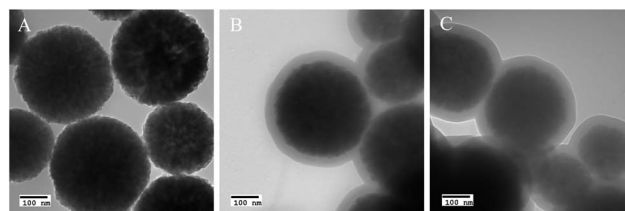


Fig. 2 Transmission electron microscopy images of Fe₃O₄ (A), Fe₃O₄@SiO₂ (B) and immobilized ALP magnetic nanoparticles (C).

literature.³⁰ The core-shell structure of Fe₃O₄@SiO₂ with a shell layer of 33 nm is obviously presented in Fig. 2B, and the thickness of the shell increased to approximately 39 nm after ALP immobilization (Fig. 2C).

FTIR spectroscopy was performed to further reveal evidence of the immobilized ALP present on the surface of magnetic nanoparticles (ESI, Fig. S2†). The peak at 1086 cm⁻¹ is assigned to the silica layer vibrations. The intense band between 3300 and 3400 cm⁻¹ results from the stretching vibration of the hydroxyl group. Compared with Fe₃O₄@SiO₂, the absorption peaks at 2926, 2865, 1632 and 1456 cm⁻¹ could be observed in the spectrum of immobilized ALP magnetic nanoparticles, which correspond to the vibrations of methylene and amide groups arose from enzyme side chains on the surface of nanoparticles. The FTIR results are closely similar to previous results described in the literature,^{7,31} and suggest that ALP was

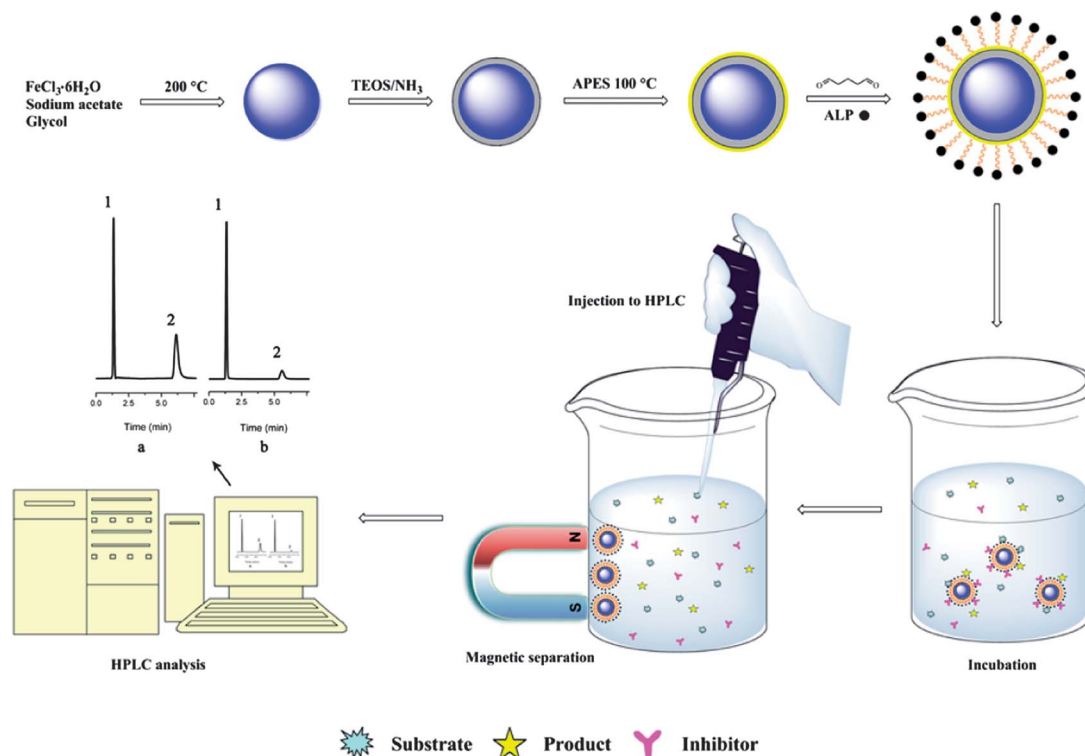


Fig. 1 Schematic of the synthesis of immobilized ALP magnetic nanoparticles and their use in an enzyme assay. Insets: typical HPLC chromatograms for the immobilized enzyme assay with no inhibition (a) and sample containing theophylline (b). Peaks (1) 4-nitrophenylphosphate and (2) 4-nitrophenol. Conditions: column, Agilent Eclipse XDB-C18 (150 × 4.6 mm i.d., 5 μm particle); detection wavelength, 311 nm; mobile phase, methanol : water (40 : 60%, v/v); flow rate, 1.0 ml min⁻¹; injection volume, 20 μl.

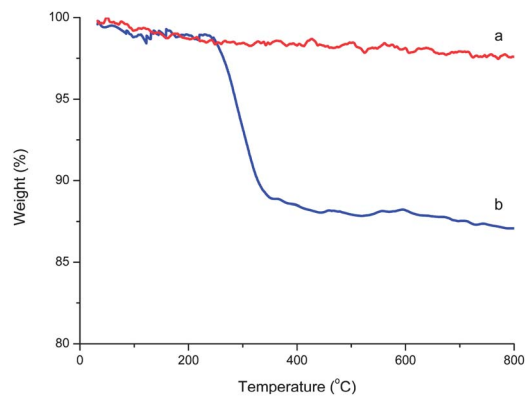


Fig. 3 TGA analysis of Fe₃O₄@SiO₂ (a) and immobilized ALP magnetic nanoparticles (b).

successfully attached to the magnetic nanoparticles. The relative enzyme binding capacity was estimated to be about 115.5 $\mu\text{g mg}^{-1}$ from the TGA result (Fig. 3).

The magnetic properties of samples were measured by applying an external magnetic field at room temperature by VSM, and the hysteresis curves are presented in Fig. 4, which confirms the superparamagnetism of these magnetite. The results showed that the saturation magnetization values of Fe₃O₄, Fe₃O₄@SiO₂ and immobilized ALP magnetic nanoparticles were 86.7, 57.2 and 47.9 emu g^{-1} respectively. A dramatic decline in magnetic response implied an increase in the thickness of the shell layer, in agreement with the results obtained above. The immobilized ALP magnetic nanoparticles could be dispersed in water by sonication or vigorous shaking, resulting in a black suspension, and were also easily aggregated from a homogeneous dispersion by an external magnet, as shown in the inset of Fig. 4. Moreover, re-dispersion occurred quickly with gentle shaking after the magnetic field was removed. These results show that the prepared nanoparticles possess remarkable magnetic responsiveness and redispersibility, which is an advantage in the separation and reuse of the immobilized enzyme in practical applications.

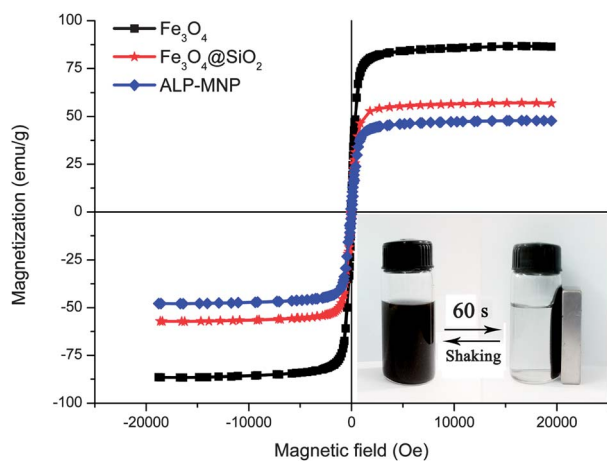


Fig. 4 Magnetization curves of Fe₃O₄, Fe₃O₄@SiO₂ and immobilized ALP magnetic nanoparticles. Inset: magnetic separation and re-dispersion of immobilized ALP magnetic nanoparticles.

3.2 Optimization of enzymolysis conditions

Control experiments were performed on the silanized magnetite (Fe₃O₄@SiO₂@APES) and the immobilized ALP magnetic nanoparticles to validate the effect of the immobilized enzyme. In the absence of immobilized ALP, only the substrate (4-nitrophenylphosphate) was observed by HPLC. In contrast, the colorless sample solution turned to yellow after treatment with immobilized ALP magnetic nanoparticles and, meanwhile, another peak could be detected and identified by its retention time as the enzymolysis product, 4-nitrophenol. This comparison indicates that the ALP immobilized on magnetic nanoparticles and not the Fe₃O₄ core catalyzed the hydrolysis of the substrate. The results further demonstrate the feasibility of the protocol for using the immobilized ALP magnetic nanoparticles and that the prepared magnetite could provide a biocompatible microenvironment that retains the major activities of enzymes.

Temperature is one of the most important factors in enzymatic hydrolysis. The results of the experiments performed between 20 and 60 °C are presented in Fig. 5A, which show that the enzymolysis efficiency initially increased with increasing temperatures up to 40 °C and that ALP was deactivated as the temperature continued to rise, leading to a dramatic decline in the enzymolysis efficiency. The optimal temperature was 40 °C. The effect of incubation time on the yield of the reaction product is shown in Fig. 5B. A longer incubation time allows the substrate to react more completely with the immobilized ALP magnetic nanoparticles. On the other hand, longer enzymolysis increases the duration of experiments. An optimal incubation time of 30 min was selected for the subsequent experiments. The effect of pH on the activity of immobilized ALP was determined from pH 8.0 to 11.0, showing a maximum at pH 9.5 (Fig. 5C).

Based on the results obtained above, the optimal substrate concentrations and the kinetic behavior of immobilized ALP were investigated. The results for magnetic nanoparticles incubated with a range of 4-nitrophenylphosphate concentrations are shown in Fig. 5D. The enzymolysis efficiency increased with increasing substrate concentrations up to 1 mg ml^{-1} .

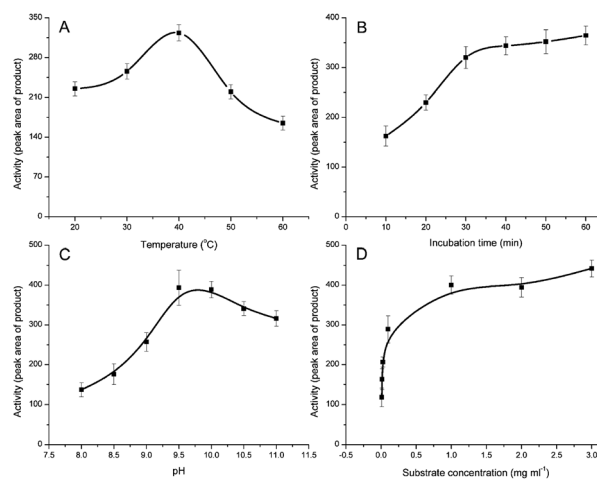


Fig. 5 (A) Effect of temperature on enzymolysis efficiency. (B) Effect of incubation time on enzymolysis efficiency. (C) Effect of pH on enzymolysis efficiency. (D) Effect of substrate concentration on enzymolysis efficiency.

However, further increases in concentration did not increase the enzymolysis efficiency significantly because the enzyme binding capacity and enzymolysis ability were saturated due to the fixed amount of ALP immobilized on the surface of the nanoparticles. The most important kinetic constant of the enzyme reaction, the Michaelis constant, can be determined by the Lineweaver–Burk method.³² The Lineweaver–Burk plot was linear and gave a Michaelis constant of 67.14 μM , similar to the results reported in the literature.²⁰ In addition, X-ray diffraction patterns of ALP show that the diffraction peak angles are similar before and after immobilization (ESI, Fig. S3[†]), which indicates that the ALP conformation has no obvious change. These results demonstrate that no significant change in enzyme properties was observed when using the proposed method.

The repeatability of the immobilized ALP magnetic nanoparticles was assessed by carrying out five sequential enzymatic hydrolyses using the same immobilized enzyme. The results show that the relative standard deviation (RSD) was 5.06%. The storage stability was assessed by measuring activity after storage in buffer at 4 °C for 30 days, and the activity remained at 80.15%. Compared with free ALPs in solution that are more susceptible to denaturation, the immobilized ALP on magnetic nanoparticles lost some activity after storage for 30 days but still retained a major enzymatic activity, enough for the subsequent experiments. Moreover, the immobilized ALP on magnetic nanoparticles allows easy manipulation and separation from reaction mixtures simply by applying a magnetic field, with no need for centrifuges or filters, which significantly removes interferences, shortens procedural time and simplifies the experimental process.

3.3 Immobilized ALP magnetic nanoparticles for enzyme inhibition study

Abnormal activity or expression of enzymes occurs with the emergence and metastasis of diseases. Enzymes are a useful class of indicators for disease diagnosis and play an important role during drug discovery processes.^{33,34} One of the most useful applications of immobilized enzyme magnetic nanoparticles is in enzyme inhibition assays. In this study, three inhibitor candidates, theophylline, L-tryptophan and D-tryptophan, were used to evaluate the function of the immobilized ALP magnetic nanoparticles.

The inhibition efficiency curves for theophylline and L-tryptophan were obtained by varying the inhibitor concentration

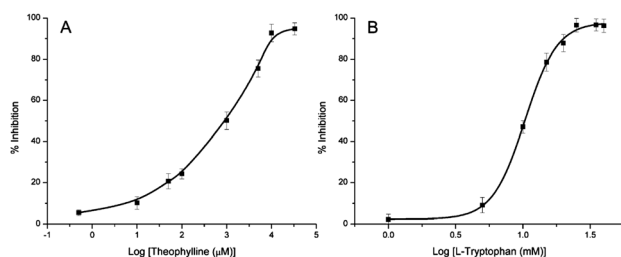


Fig. 6 Inhibition efficiency curves for the immobilized ALP magnetic nanoparticles in the presence of inhibitors. (A) Theophylline and (B) L-tryptophan.

(maintaining a constant substrate concentration), as shown in shown in Fig. 6. The results show that the IC_{50} value for theophylline was 0.71 mM and clearly smaller than that for L-tryptophan (10.32 mM), which suggests that theophylline has a markedly stronger inhibitive effect. In contrast to the absence of inhibitor (inset (a) of Fig. 1), inset (b) of Fig. 1 represents an ALP inhibition assay in which theophylline was added, showing a dramatic reduction in the product peak area. The inhibition constant K_i for the two inhibitors at IC_{50} was also determined to be 0.276 mM (theophylline) and 6.07 mM (L-tryptophan). The K_i values reported here are higher than those obtained with free ALP in solution,³⁵ reflecting improved stability and resistance to inhibition by immobilized ALP. Compared with L-tryptophan, D-tryptophan did not display obvious inhibition, which suggests that DL-tryptophan possesses a chirally dependent inhibition for ALP. This may be because the inhibitor recognition site is commonly located within a groove or crack in the enzyme structure. Thus, only an inhibitor that possesses a suitable spatial structure can bind to the enzyme and exhibit an inhibitory effect.³⁶

The enzyme inhibitive kinetics was investigated for the immobilized ALP magnetic nanoparticles using the optimal enzymolysis conditions described above. The Lineweaver–Burk plots were obtained at different inhibitor concentrations for both inhibitors (theophylline and L-tryptophan). Fig. 7A shows

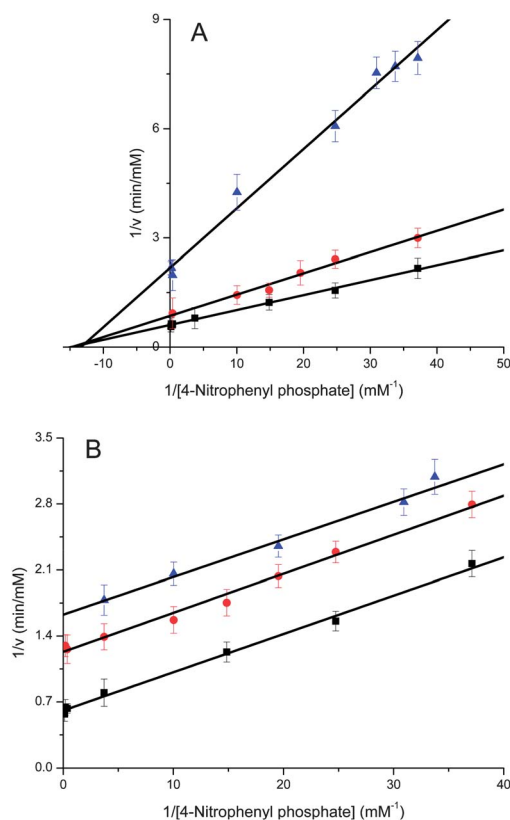


Fig. 7 (A) Lineweaver–Burk plot for the immobilized ALP magnetic nanoparticles in the presence of theophylline at various concentrations. Conditions: (■) 0 mM; (●) 0.1 mM; (▲) 1 mM. (B) Lineweaver–Burk plot for the immobilized ALP magnetic nanoparticles in the presence of L-tryptophan at various concentrations. Conditions: (■) 0 mM; (●) 5 mM; (▲) 10 mM.

that the maximum enzymolysis velocity declined with the increasing concentration of theophylline, whereas the Michaelis constant barely changed. This corresponds to the characteristics of noncompetitive inhibition and demonstrates that theophylline is a noncompetitive inhibitor for ALP. The Lineweaver–Burk curves for L-tryptophan exhibit that as the inhibitor concentration increased, the maximum enzymolysis velocity and Michaelis constant both declined but their ratio was constant, showing a series of parallel straight lines in Fig. 7B. These results indicate that L-tryptophan displayed an uncompetitive inhibition behavior.

4 Conclusions

A new strategy using ALP immobilized onto magnetic nanoparticles for enzymolysis and enzyme inhibition assays has been developed. The formation of the prepared immobilized ALP magnetic nanoparticles was confirmed by various characterization techniques and exhibited a clear three-dimensional core–shell architecture and high saturation magnetization. A practical application of the enzymatic hydrolysis and enzyme inhibition assay was performed to evaluate the immobilized ALP magnetic nanoparticles. The results demonstrate that they possess high enzymolysis efficiency and satisfactory repeatability. This method combines the advantages of immobilized enzymes and magnetic media so that it not only offers low cost through re-use of enzyme but also allows fast and simple separation using magnets. The protocol provides a facile and efficient approach to the fabrication of magnetic core/functionalized ALP shell hierarchical structures, which can be easily adapted to immobilization of other enzymes and potentially realize high-throughput screening of enzyme reactions and enzyme inhibitors.

Acknowledgements

This work was supported by the National Natural Science Foundation of China (no. 21075008 and 90713013).

Notes and references

- 1 F. X. Qie, G. X. Zhang, J. X. Hou, X. M. Sun, S. Z. Luo and T. W. Tan, *Talanta*, 2012, **93**, 166–171.
- 2 R. Hao, R. J. Xing, Z. C. Xu, Y. L. Hou, S. Gao and S. H. Sun, *Adv. Mater.*, 2010, **22**, 2729–2742.
- 3 H. M. Chen, C. H. Deng and X. M. Zhang, *Angew. Chem., Int. Ed.*, 2010, **122**, 617–621.
- 4 C. E. Probst, P. Vrazhevskiy and X. H. Gao, *J. Am. Chem. Soc.*, 2011, **133**, 17126–17129.
- 5 M. Kalantari, M. Kazemeini, F. Tabandeh and A. Arpanaei, *J. Mater. Chem.*, 2012, **22**, 8385–8393.
- 6 S. A. Ansari and Q. Husain, *Biotechnol. Adv.*, 2012, **30**, 512–523.
- 7 K. Khoshnevisan, A. K. Bordbar, D. Zare, D. Davoodi, M. Noruzi, M. Barkhi and M. Tabatabaei, *Chem. Eng. J.*, 2011, **171**, 669–673.
- 8 E. Ranjbakhsh, A. K. Bordbar, M. Abbasi, A. R. Khosropour and E. Shams, *Chem. Eng. J.*, 2012, **179**, 272–276.
- 9 H. M. Chen, S. S. Liu, H. L. Yang, Y. Mao, C. H. Deng, X. M. Zhang and P. Y. Yang, *Proteomics*, 2010, **10**, 930–939.
- 10 S. Lin, D. Yun, D. W. Qi, C. H. Deng, Y. Li and X. M. Zhang, *J. Proteome Res.*, 2008, **7**, 1297–1307.
- 11 X. Y. Yan and S. D. Gilman, *Electrophoresis*, 2010, **31**, 346–354.
- 12 A. H. Lu, E. L. Salabas and F. Schuth, *Angew. Chem., Int. Ed.*, 2007, **46**, 1222–1244.
- 13 R. Villalonga, M. L. Villalonga, P. Diez and J. M. Pingarron, *J. Mater. Chem.*, 2011, **21**, 12858–12864.
- 14 L. S. Qing, Y. Xue, Y. Zheng, J. Xiong, X. Liao, L. S. Ding, B. G. Li and Y. M. Liu, *J. Chromatogr., A*, 2010, **1217**, 4663–4668.
- 15 F. L. Hu, H. Y. Zhang, H. Q. Lin, C. H. Deng and X. M. Zhang, *J. Am. Soc. Mass Spectrom.*, 2008, **19**, 865–873.
- 16 J. P. Lalles, *Nutr. Rev.*, 2010, **68**, 323–332.
- 17 T. D. Y. Chung, E. Sergienko and J. L. Millan, *Molecules*, 2010, **15**, 3010–3037.
- 18 F. G. Sanchez, A. N. Diaz, M. C. R. Peinado and C. Belledone, *Anal. Chim. Acta*, 2003, **484**, 45–51.
- 19 S. Sidique, R. Ardecky, Y. Su, S. Narisawa, B. Brown, J. L. Millan, E. Sergienko and N. D. P. Cosford, *Bioorg. Med. Chem. Lett.*, 2009, **19**, 222–225.
- 20 J. Iqbal, *Anal. Biochem.*, 2011, **414**, 226–231.
- 21 S. M. Wang, P. Su and Y. Yang, *Anal. Biochem.*, 2012, **427**, 139–143.
- 22 S. M. Wang, P. Su, E. Hongjun and Y. Yang, *Anal. Biochem.*, 2010, **405**, 230–235.
- 23 J. B. Zhang, H. H. Yan, T. Yang and Y. R. Zong, *J. Environ. Manage.*, 2011, **92**, 53–58.
- 24 T. B. Goriushkina, A. P. Soldatkin and S. V. Dzyadevych, *J. Agric. Food Chem.*, 2009, **57**, 6528–6535.
- 25 L. Yang, C. Y. Chen, Y. F. Chen, J. Shi, S. D. Liu, L. P. Guo and H. F. Xu, *Anal. Chim. Acta*, 2010, **683**, 136–142.
- 26 Z. Liu, H. S. Wang, B. Li, C. Liu, Y. J. Jiang, G. Yu and X. D. Mu, *J. Mater. Chem.*, 2012, **22**, 15085–15091.
- 27 H. Deng, X. L. Li, Q. Peng, X. Wang, J. P. Chen and Y. D. Li, *Angew. Chem., Int. Ed.*, 2005, **44**, 2782–2785.
- 28 H. L. Wang, J. J. Cao, Y. P. Bi, L. Chen and Q. H. Wan, *J. Chromatogr., A*, 2009, **1216**, 5882–5887.
- 29 E. Akyilmaz and M. Turemis, *Electrochim. Acta*, 2010, **55**, 5195–5199.
- 30 Y. Wei, A. L. Tian, Y. Li, X. Wang and B. Cao, *J. Mater. Chem.*, 2012, **22**, 8499–8504.
- 31 K. Ashtari, K. Khajeh, J. Fasihi, P. Ashtari, A. Ramazani and H. Vali, *Int. J. Biol. Macromol.*, 2012, **50**, 1063–1069.
- 32 J. Saevels, K. Van den Steen, A. Van Schepdael and J. Hoogmartens, *J. Chromatogr., A*, 1996, **745**, 293–298.
- 33 S. M. Fang, H. N. Wang, Z. X. Zhao and W. H. Wang, *J. Pharm. Anal.*, 2012, **2**, 83–89.
- 34 Z. M. Tang and J. W. Kang, *Anal. Chem.*, 2006, **78**, 2514–2520.
- 35 A. R. Whisnant and S. D. Gilman, *Anal. Biochem.*, 2002, **307**, 226–234.
- 36 C. W. Lin, H. G. Sie and W. H. Fishman, *Biochem. J.*, 1971, **124**, 509–516.